STF-based diagnosis of AUV thruster faults

Chunmeng Jiang, *Jinhua* Lv*, *Yanli* Liu, *Gaoyang* Wang, *Xin* Xu, and *Ying* Deng

Wuhan Institute of Shipbuilding Technology, Wuhan, 430050, China

Abstract. The diagnosis of thruster faults of autonomous underwater vehicles is studied in this paper. Based on the theory of strong tracking filter (STF), the AUV motion model and the thruster fault model are established. The STFs are designed for each thruster for the purpose of fault diagnosis. The AUV state and the fault deviation of the thruster are estimated online before the thruster faults are diagnosed based on residual analysis. The simulation experiments were conducted to verify the feasibility and effectiveness of the STF-based diagnosis of AUV thruster faults.

Keywords: Autonomous underwater vehicle, Fault diagnosis, Strong track filter, Thruster.

1 Introduction

The urgent needs in marine resource exploration in recent years have boosted the rapid development of underwater vehicles and relevant technologies, especially autonomous underwater vehicles (AUV). AUVs are free from entangled cables or support from the surface system and distinguished with wide range of activities, admirable diving depth, little requirement on deck area, low cost and the ability to access complex environment[1-2]. With the growing degree of autonomy, increasing numbers of control system as well as more eminent performance, AUVs have become capable with more and more complex tasks. For this reason, higher requirements have been put forward on the AUV reliability with the expectation that any fault can be detected and isolated immediately.

The ability of fault diagnosis is a must for AUVs to successfully complete operation tasks in unknown marine environment of high pressure and poor visibility. Present methods for fault diagnosis are primarily based on analytic model, signal processing and artificial intelligence[3-4]. In this paper, the theory of strong tracking filter is adopted to monitor and diagnose AUV thruster faults.

2 AUV profile

The research object in this paper is a multi-functional autonomous underwater vehicle as shown in Figure 1. It realizes functions of motion control, fault diagnosis, long-range

* Corresponding author: 2061770742@qq.com

navigation, submarine terrain mapping, dam detection and target recognition[5]. To satisfy the requirements above, the AUV is designed with a streamlined profile together with stabilizers for improved stability.

The AUV is composed of autonomous planning system, navigation system, control system, target detection system and emergency system[6]. The planning system gives target instructions, the navigation systems providing location data, the control system realizing closed-loop control according to the target instruction, the target detection system collecting data of the target or obstacle and the emergency system complementing self-rescue. For the purpose of coming-up in the event of power or computer failure, the AUV is designed with slightly greater buoyancy than gravity.

The propulsion system is made up of four thrusters and accessories involved, including two conduit thrusters and two slot thrusters. The two conduit thrusters on each side of the stern serve as the left thruster and the right thruster respectively. The two slot thrusters at the bow and the stern serve as the side thrusters.

Fig.1. Profile of the AUV.

3 Strong tracking filter

Extended Kalman Filter (EKF) is adopted to estimate the following discrete state space models.

$$x(k+1) = f(k, u(k), x(k)) + \Gamma(k)v(k) \tag{1}$$

$$y(k+1) = h(k+1, x(k+1)) + e(k+1) \tag{2}$$

With highly precise models as expressed above and appropriate initial values of $\hat{x}(0|0)$ and $P(0|0)$ for the filter, the EKF provide accurate state estimate $\hat{x}(k+1|k+1)$. However, EKF is subject to poor robustness to model uncertainties. In case of inaccurate model, the state estimates would be deviating or even divergent. In addition, EKF will lose tracking of the changing system when reaching the steady state.

In order to overcome the defects of EKF, a filter with better performance is needed. The strong tracking filter is hereby introduced due to its strong robustness to the variation of actual system parameters, low sensitivity to system noise, measurement noise and initial values, as well as outstanding ability of tracking mutating state. Also, EKF remains its ability of tracking slowly or sharply changed state when it enters the steady state.

The STF is expected of strong robustness to the above model uncertainties and continuous tracking ability. To realize the outstanding tracking characteristics, a sufficient condition that distinguishes a general filter to a STF is online selection of time-varying gain (TVG) matrix, so that

$$E[x(k+1) - \hat{x}(k+1|k+1)][x(k+1) - \hat{x}(k+1)]^T = \min \tag{3}$$

$$E[\gamma^T(k+1)\gamma(k+1+j)]=0, k=0,1,2,\cdots, j=1,2,\cdots \tag{4}$$

where Equation (3) requires the minimum variance of state estimation residual while Equation (4) outputs all-the-time orthogonal residual sequence.

For the purpose of admirable tracking ability, fading factor can be used to rule out historical data, and real-time adjustment should be made on the covariance matrix and corresponding gain matrix of state prediction error. Therefore, the fading factor λ is introduced, hence the Suboptimal Fading Extended Kalman Filter (SFEKF) as follows,

$$\hat{x}(k+1\mid k+1)=\hat{x}(k+1\mid k)+K(k+1)\gamma(k+1) \tag{5}$$

where

$$\hat{x}(k+1\mid k)=f(k,u(k),\hat{x}(k\mid k) \tag{6}$$

$$\begin{aligned}K(k+1)=P(k+1\mid k)H^T(k+1,\hat{x}(k+1\mid k))[H(k+1),\hat{x}(k+1\mid k))\\ \times P(k+1\mid k)H^T(k+1,\hat{x}(k+1\mid k))+R(k+1)]^{-1}\end{aligned} \tag{7}$$

$$\begin{aligned}P(k+1\mid k)=\lambda(k+1)F(k,u(k),\hat{x}(k\mid k))P(k\mid k)F^T(k,u(k),\hat{x}(k\mid k))\\ +\Gamma(k)Q(k)\Gamma^T(k)\end{aligned} \tag{8}$$

$$P(k+1\mid k+1)=[I-K(k+1)H(k+1,\hat{x}(k+1\mid k))]P(k+1\mid k) \tag{9}$$

$$\gamma(k+1)=y(k+1)-\hat{y}(k+1)=y(k+1)-h(k+1,\hat{x}(k+1\mid k)) \tag{10}$$

$$H(k+1,\hat{x}(k+1\mid k)=\left.\frac{\partial h(k+1,x(k+1))}{\partial x}\right|_{x(k+1)=\hat{x}(k+1\mid k)} \tag{11}$$

$$F(k,u(k),\hat{x}(k\mid k)=\left.\frac{\partial f(k,u(k)x(k))}{\partial x}\right|_{x(k)=\hat{x}(k\mid k)} \tag{12}$$

The mean squared error matrix is

$$\begin{aligned}V_0(k+1)&=E[\gamma(k+1)\gamma^T(k+1)]\\ &\approx H(k+1,\hat{x}(k+1\mid k))P(k+1\mid k)H^T(k+1,\hat{x}(k+1\mid k))+Q_2(k+1)\end{aligned} \tag{13}$$

The suboptimal fading factor $\lambda(k+1)$ can be approximated by Equation (14)

$$\lambda(k+1)=\begin{cases}\lambda_0, & \lambda_0\geq 1\\ 1, & \lambda_0<1\end{cases} \tag{14}$$

where

$$\lambda_0 = \frac{tr[N(k+1)]}{tr[M(k+1)]} \tag{15}$$

$$\begin{aligned} N(k+1) &= V_0(k+1) - H(k+1,\hat{x}(k+1\,|\,k)\Gamma(k)Q_1(k)\Gamma^T(k) \\ &\times H^T(k+1,\hat{x}(k+1\,|\,k)) - Q_2(k+1) \end{aligned} \tag{16}$$

$$\begin{aligned} M(k+1) &= H(k+1,\hat{x}(k+1\,|\,k))F(k,u(k),\hat{x}(k\,|\,k))P(k\,|\,k) \\ &\times F^T(k,u(k),\hat{x}(k\,|\,k))H^T(k+1,\hat{x}(k+1\,|\,k)) \end{aligned} \tag{17}$$

4 AUV Fault diagnosis

4.1 AUV Motion Model

With the models in Equations (1) and (2), the state variables are defined as

$$x = \begin{bmatrix} x_1 & x_2 & x_3 \end{bmatrix}^T = \begin{bmatrix} u & v & r \end{bmatrix}^T \tag{18}$$

In addition, system output variables are

$$y = [y_1 \quad y_2 \quad y_3]^T = \begin{bmatrix} u & v & r \end{bmatrix}^T \tag{19}$$

and system input variables are

$$u = \begin{bmatrix} u_1 & u_1 & u_1 \end{bmatrix}^T = \begin{bmatrix} X_T & Y_T & N_T \end{bmatrix}^T \tag{20}$$

At this point the AUV model is

$$\begin{cases} x(k+1) = f(k,u(k),x(k)) \\ y(k+1) = G \cdot x(k+1) + e(k+1) \end{cases} \tag{21}$$

$$f(k,u(k),x(k)) = \begin{bmatrix} x_1(k) + T\dfrac{X_f(k)}{A} \\ x_2(k) + T\dfrac{Y_f(k)\cdot D - N_f(k)\cdot C}{P} \\ x_3(k) + T\dfrac{N_f(k)\cdot B - Y_f(k)\cdot E}{P} \end{bmatrix} \tag{22}$$

$$G = \begin{bmatrix} 1 & 0 & 0 \\ 0 & 1 & 0 \\ 0 & 0 & 1 \end{bmatrix} \tag{23}$$

where $A = m - X_{\dot{u}}$, $B = m - Y_{\dot{v}}$, $C = mx_G - Y_{\dot{r}}$, $D = I_z - N_{\dot{r}}$, $E = mx_G - N_{\dot{v}}$, $P = BD - CE = (m - Y_{\dot{v}})(I_z - N_{\dot{r}}) - (mx_G - Y_{\dot{r}})(mx_G - N_{\dot{v}})$.

$$\begin{aligned} X_f(k) = {} & mx_2(k)x_3(k) + mx_G x_3^2(k) + X_{uu}x_1^2(k) + \\ & + X_{vr}x_2(k)x_3(k) + X_{rr}x_3^2(k) + u_1 + u_4 \end{aligned} \tag{24}$$

$$\begin{aligned} Y_f(k) = {} & -mx_1(k)x_3(k) + Y_v x_1(k)x_2(k) + Y_r x_1(k)x_3(k) \\ & + Y_{v|v|}x_2(k)\left|x_2(k)\right| + Y_{v|r|}x_2(k)\left|x_3(k)\right| + Y_{r|r|}x_3(k)\left|x_3(k)\right| + u_2 + u_5 \end{aligned} \tag{25}$$

$$\begin{aligned} N_f(k) = {} & -mx_G x_1(k)x_3(k) + N_v x_1(k)x_2(k) + N_r x_1(k)x_3(k) \\ & + N_{v|v|}x_2(k)\left|x_2(k)\right| + N_{v|r|}x_2(k)\left|x_3(k)\right| + N_{r|r|}x_3(k)\left|x_3(k)\right| + u_3 + u_6 \end{aligned} \tag{26}$$

4.2 Thruster fault model

X_T^*, Y_T^* and N_T^* are the expected thrusting force in each degree of freedom. T_{ML}^*, T_{MR}^*, T_{HB}^* and T_{HS}^* are the expected thrusting force respectively provided by the left thruster, right thruster, side thruster at the bow and side thruster at the stern, with l_M, l_M, l_{HB} and l_{HS} the force arms to the center of the AUV body.

$$\begin{cases} T_{ML}^* = T_{MR}^* = 0.5X_T^* \\ T_{HB}^* = \dfrac{Y_T^* \cdot l_{HS}}{l_{HB} + l_{HS}} + \dfrac{N_T^*}{l_{HB} + l_{HS}} \\ T_{HS}^* = \dfrac{Y_T^* \cdot l_{HB}}{l_{HB} + l_{HS}} - \dfrac{N_T^*}{l_{HB} + l_{HS}} \end{cases} \tag{27}$$

When there is no thruster fault, the expected thrusting forces are

$$\begin{cases} T_{ML} = T_{ML}^* \\ T_{MR} = T_{MR}^* \\ T_{HB} = T_{HB}^* \\ T_{HS} = T_{HS}^* \end{cases} \tag{28}$$

$$\begin{cases} X_T = X_T^* \\ Y_T = Y_T^* \\ N_T = N_T^* \end{cases} \tag{29}$$

In case of fault on the left thruster, $T_{ML} = 0$,

$$\begin{cases} X_T = 0.5X_T^* \\ Y_T = Y_T^* \\ N_T = N_T^* - T_{MR}l_M = N_T^* - 0.5X_T^* l_M \end{cases} \tag{30}$$

In case of fault on the right thruster, $T_{MR}=0$,

$$\begin{cases} X_T = 0.5X_T^* \\ Y_T = Y_T^* \\ N_T = N_T^* + T_{MR}l_M = N_T^* + 0.5X_T^*l_M \end{cases} \tag{31}$$

In case of fault on the side thruster at the bow, $T_{HB}=0$,

$$\begin{cases} X_T = X_T^* \\ Y_T = T_{HS} = \dfrac{Y_T^* \cdot l_{HB}}{l_{HB}+l_{HS}} - \dfrac{N_T^*}{l_{HB}+l_{HS}} \\ N_T = T_{HS}l_{HS} = (\dfrac{Y_T^* \cdot l_{HB}}{l_{HB}+l_{HS}} - \dfrac{N_T^*}{l_{HB}+l_{HS}})l_{HS} \end{cases} \tag{32}$$

In case of fault on the side thruster at the stern, $T_{HS}=0$,

$$\begin{cases} X_T = X_T^* \\ Y_T = T_{HB} = \dfrac{Y_T^* \cdot l_{HS}}{l_{HB}+l_{HS}} + \dfrac{N_T^*}{l_{HB}+l_{HS}} \\ N_T = T_{HB}l_{HB} = (\dfrac{Y_T^* \cdot l_{HS}}{l_{HB}+l_{HS}} + \dfrac{N_T^*}{l_{HB}+l_{HS}})l_{HB} \end{cases} \tag{33}$$

4.3 Fault diagnosis principle and simulation results

Based on the motion model of the AUV, STFs are designed for fault diagnosis of each thruster. The comparison between the estimates and actual values of the five STFs leads to five groups of residual values. The analysis and comparison of the residual values will immediately give the failed thruster. Simulation experiments were carried out according to the above method, and residual errors were analyzed, which revealed the relation between residual errors and thruster fault.

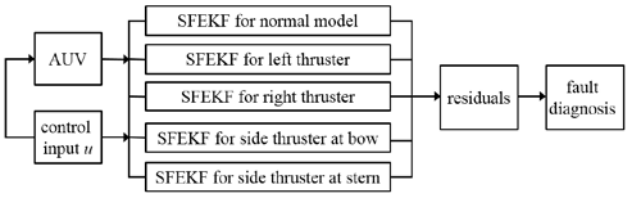

Fig.2. Principle of thruster fault diagnosis.

In the simulation experiment, the left thruster suffered from step fault at the 200th second. The residual analysis was expected to diagnose the fault situation. It is obvious in Figure 3 and Figure 4 that at 200s, the left thruster and the right thruster in the fault model showed equal residuals of velocity in the surge direction and both were smaller than that in the normal model. It indicated failure of the main thrusters at 200s (due to the jump of velocity residual). In addition, the residual of velocity in the yaw dimension further

attributed the failure to the left thruster because the left thruster showed the smallest residual of the velocity in the yaw dimension after 200s.

The simulation results verified STF's high estimation precision and insensitivity to initial values. In case of thruster failure, STF can track the actual speed immediately and remain high tracking precision, together with the ability to evaluate the failure situation and keep the failure isolated.

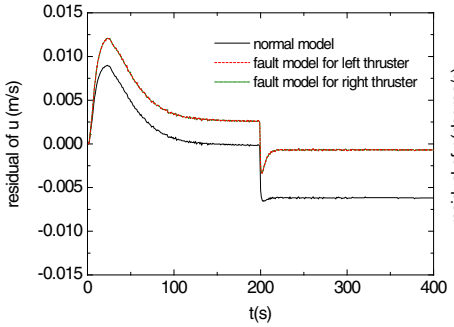

Fig.3. Residual of velocity *u* upon left thruster fault.

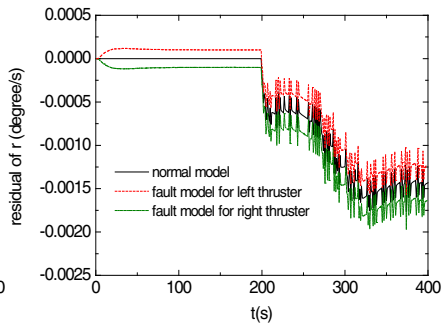

Fig.4. Residual of velocity *r* upon left thruster fault.

5 Conclusions

The feasibility of the application of strong tracking filter in AUV thruster fault diagnosis is discussed in this paper. Simulation experiments have verified the effectiveness of the STF-based method for fault diagnosis which also satisfies the detection and diagnosis of sensor step faults. Further studies will focus on the reliability of fault diagnosis based on the proposed method.

This work was financially supported by National Natural Science Foundation of China (No. 51709061).

Reference

1. Ji Daxiong, Yao Xin, Li Shuo, Tang Yuangui, Tian Yu. Autonomous underwater vehicle fault diagnosis dataset [J]. Data in Brief, 2021, 39: 107477-107477.
2. Xia Shaoxuan, Zhou Xiaofeng, Shi Haibo et al. A fault diagnosis method based on attention mechanism with application in Qianlong-2 autonomous underwater vehicle[J]Ocean Engineering, 2021, 233
3. Yu Caoyang, Zhong Yiming, Lian Lian et al. An experimental study of adaptive bounded depth control for underwater vehicles subject to thruster's dead-zone and saturation[J] Applied Ocean Research, 2021, 117
4. Yu Dacheng,Zhu Chenguang,Zhang Mingjun,Liu Xing. Experimental Study on Multi-Domain Fault Features of AUV with Weak Thruster Fault[J]. Machines,2022,10(4): 236-236.
5. Jiang Chunmeng. The Application of PSO-AFSA Method in Parameter Optimization for Underactuated Autonomous Underwater Vehicle Control[J]. Mathematical Problems in Engineering, 2017, 8: 1-14
6. Jiang Chunmeng. Design of Novel Sliding-Mode Controller for High-Velocity AUV with Consideration of Residual Dead Load[J]. Journal of Central South University, 2018, 25(1): 121-130